

Understanding of the Common Land Model performance for water and energy fluxes in a farmland during the growing season in Korea

Minha Choi,¹ Seung Oh Lee^{2*} and Hyojung Kwon³

¹ Department of Civil and Environmental Engineering, Hanyang University, Seoul 133-791, Republic of Korea

² School of Urban and Civil Engineering, Hongik University, Seoul 121-791, Republic of Korea

³ Department of Atmospheric Sciences, Yonsei University, Seoul 120-749, Republic of Korea

Abstract:

The Common Land Model (CLM) is one of the most widely used land surface models (LSMs) due to the practicality of its simple parameterization scheme and its versatility in embracing a variety of field datasets. The improved assessment of land surface water and energy fluxes using CLM can be an alternative approach for understanding the complex land–atmosphere interactions in data-limited regions. The understanding of water and energy cycles in a farmland is crucial because it is a dominant land feature in Korea and Asia. However, the applications of CLM to farmland in Korea are in paucity. The simulations of water and energy fluxes by CLM were conducted against those from the tower-based measurements during the growing season of 2006 at the Haenam site (a farmland site) in Korea without optimization. According to the International Geosphere–Biosphere Programme (IGBP) land cover classification, a homogeneous cropland was selected initially for this study. Although the simulated soil moisture had a similar pattern to that of the observed, the former was relatively drier (at $0.1 \text{ m}^3 \text{ m}^{-3}$) than the latter. The simulated net radiation showed good agreement with the observed, with a root mean squared error (RMSE) of 41 W m^{-2} , whereas relatively large discrepancies between the simulation and observation were found in sensible (RMSE of 66 W m^{-2}) and latent (RMSE of 60 W m^{-2}) heat fluxes. On the basis of the sensitivity analysis, soil moisture was more receptive to land cover and soil texture parameterizations when compared to soil temperature and turbulent fluxes. Despite the uncertainty in the predictive capability of CLM employed without optimization, the initial performance of CLM suggests usefulness in a data-limited heterogeneous farmland in Korea. Further studies are required to identify the controls on water and energy fluxes with an improved parameterization. Copyright © 2010 John Wiley & Sons, Ltd.

KEY WORDS Common Land Model; farmland; water and energy fluxes; parameterization

Received 11 July 2009; Accepted 4 November 2009

INTRODUCTION

The accurate assessment of water and energy fluxes, including water storage, is essential to understand the complex interactions between land surface and the atmosphere (Kustas *et al.*, 1996; Moulin *et al.*, 1998). Surface–vegetation–atmosphere transfer (SVAT) models have been commonly used to replicate land surface water and energy fluxes at regional and watershed scales (Liang *et al.*, 1998; Lohmann *et al.*, 1998; Dai *et al.*, 2003). During the past few decades, parameterization of the land surface schemes in SVAT models has been intensively calibrated by many previous studies (Liang *et al.*, 1998; Lohmann *et al.*, 1998; Yang *et al.*, 1995). While more physical parameterization is required for more accurate flux estimations, an untuned SVAT parameter scheme might be worth probing and applying to data-limited regions (Mohr *et al.*, 2000).

The parameterization of the Common Land Model (CLM), one of the most widely used SVAT models, is

identified as a simple scheme that requires fewer user-defined variables compared to the parameterization of other SVAT models (Dai *et al.*, 2003; Whitfield *et al.*, 2006; Choi *et al.*, 2008). In spite of its simple parameterization scheme, CLM has been used successfully to realistically simulate the seasonal variability of water (e.g. runoff) and energy dynamics over a catchment in Russia and forest sites in southwestern Amazonia (Dai *et al.*, 2003). Whitfield *et al.* (2006) showed that CLM simulations were in excellent agreement with the measured flux data at the field scale in the Prairie wetland of the south-eastern United States.

Apart from actual major field experiments, ground-based measurements are not always available to facilitate model parameterizations. Thus, the application of the CLM over a range of field conditions without specific optimization may improve our understanding of land–atmosphere interactions in data-limited regions.

In situ sampling of water and energy components is required for the validation of the CLM, particularly regarding the interpretation of water and energy dynamics at a range of field scales. During the past several years, the global flux network, consisting of more than 400 sites, has been operated using an eddy

* Correspondence to: Seung Oh Lee, School of Urban and Civil Engineering, Hongik University, Seoul 121-791, Republic of Korea.
E-mail: seungoh.lee@hongik.ac.kr

covariance system to measure the exchanges of carbon, water, and energy between the land surface and the atmosphere in America, Europe, Canada, Asia, and Australia (Baldocchi *et al.*, 2001). These flux networks provide continuous flux measurements over different ecosystem types with various temporal and spatial scales (<http://daac.ornl.gov/FLUXNET/>). As a part of the global flux network, the Korean regional flux monitoring network (KoFlux) has been established in different land covers such as forest and farmland (Kim *et al.*, 2002). The KoFlux has not only provided continuous flux data (e.g. carbon, water, and energy) but also key meteorological variables (e.g. radiation, precipitation, and soil moisture). The KoFlux sites, because of their unique hydrometeorological conditions, provide a testbed to validate the proposed use of SVAT models in order to better understand hydrometeorological processes on regional scales.

In this study, the Haeman KoFlux site (i.e. a farmland site) was selected to understand the performance of CLM as currently employed in the enhanced land information system (LIS) of the Goddard Space Flight Center (GSFC), NASA (<http://lis.gsfc.nasa.gov>). The LIS is a modelling framework consisting of several land surface models (LSMs) created to predict land surface–atmosphere interactions on a global scale (Kumar *et al.*, 2006). This study provides an initial test for CLM through replication of water and energy fluxes in a specific field condition, a heterogeneous farmland without optimization, and investigates the sensitivity of CLM performance to parameters and/or initializations in order

to provide better performance of the water and energy fluxes on a prevailing land cover type in Korea.

STUDY AREA AND DATA

The Haenam KoFlux site is located in the south-western area of the Korean Peninsula (Figure 1). The geographical information and site characteristics are described in Table I. The climate is humid and the average annual rainfall ranges from 900 to 1700 mm (Lee *et al.*, 2008). The most intensive rainfall usually occurs during summer, which accounts for approximately two-third of the annual total. Soils are categorized from silt loam to loams and the topography is almost flat on a regional scale (Lee *et al.*, 2003). The land cover is characterized by a mixture of croplands such as rice paddies, soybeans, and sweet potatoes. Rice paddies and other crops are cultivated within a few hundred metres east and west of the flux tower (Kwon *et al.*, 2009).

The eddy covariance technique was used to measure energy fluxes from a tower height of 20 m at the Haenam KoFlux site. The wind velocity and temperature were measured with a three-dimensional sonic anemometer (Model CSAT3, Campbell Scientific Inc., Logan, Utah, USA) at 10 Hz sampling rates. To measure the latent heat flux, an open-path, infrared gas analyser (IRGA; Model LI-7500, LI-COR, Inc., Lincoln, Nebraska, USA) was used. The collected data were stored into a datalogger (Model CR-5000, Campbell Scientific Inc.). A planar fit rotation (PFR) was applied to determine the angles

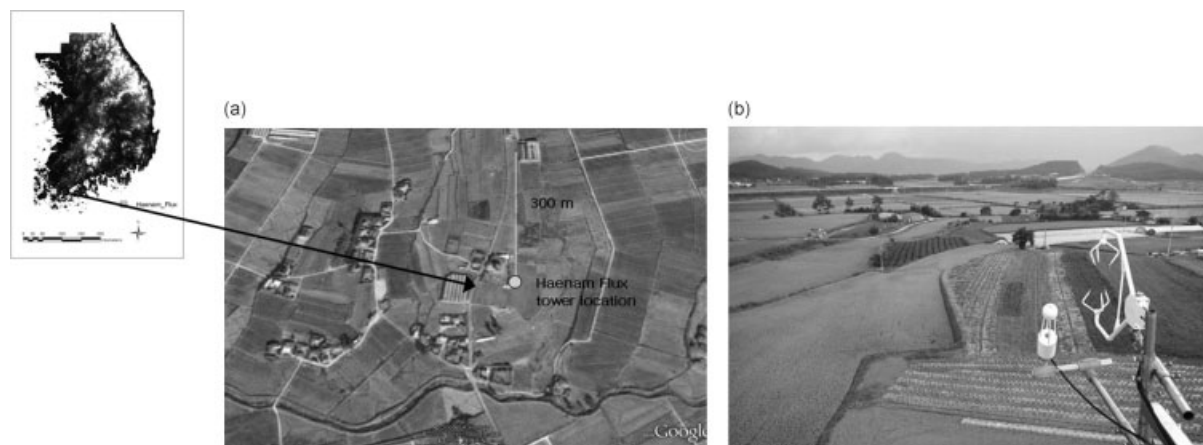


Figure 1. Study area: (a) an aerial map obtained from Google Earth (Google Local, accessed May 2009, <http://www.google.com>) and (b) the Haenam flux tower

Table I. Geographic location and site characteristics for the Haenam KoFlux site, Korea

Sites	Latitude and longitude	Study period	Land cover	Soil type	Mean annual precipitation ^a (mm)	Mean annual temperature ^a (°C)	Terrain
Haenam	34-55°N 126-56°W	6/23–7/08/2006	Rice paddy/farm land	Loam (sand 38.5%, clay 30.0%)	1306	13.3	Relatively flat

^a Source from Lee *et al.* (2008).

necessary to place the sonic anemometer into a stream-wise coordinate system (i.e. natural wind system; Wilczak *et al.*, 2001).

Other meteorological measurements were also conducted and stored in a datalogger (Model CR-5000, Campbell Scientific Inc.). The net radiation (R_n) was measured using a net radiometer (Model CNR1, Kipp & Zonen, Delft, the Netherlands) at 15 m height. The soil temperature (T_s) was measured using soil temperature probes (Model TCAV, Campbell Scientific Inc.) at a depth of 10 cm. The soil moisture content was measured with a soil moisture probe (Model CS616, Campbell Scientific Inc.) from 0 to 10 cm at two different locations, which were about 7 m apart and had similar soil conditions. Precipitation was obtained from an on-site automated weather station operated by the Korea Meteorological Administration.

The quality of the collected data was examined before the analysis to eliminate undesirable data and to improve its overall quality. We applied a quality control (QC) procedure based on micrometeorological theories and statistical tests (e.g. coordinate rotation, the control of ranges and spikes, and quality flagging; see Kwon *et al.* (2007) and Hong *et al.* (2009) for more detailed information). The study was focused on the growing season of June and July in 2006, due to continual data collection with a higher data retrieval rate after QC, therefore a gap-filling effort was not undertaken in this study.

COMMON LAND MODEL

CLM was developed through a multi-disciplinary project by combining three existing models: the LSM, the biosphere–atmosphere transfer scheme (BATS), and the Chinese Academy of Sciences Institute of Atmospheric Physics LSM (Dai *et al.*, 2003). The major characteristics of the CLM are as follows: (1) soil moistures and soil temperatures are calculated within 10 uneven layers; (2) snow pack can also be calculated in multi-layers; (3) calculations of runoff and infiltration are based on basic TOPMODEL concepts assuming that the saturated hydraulic conductivity decreases exponentially (Beven and Kirkby, 1979); and (4) energy and water balances are calculated in a tile divided by every sub-grid fraction. Each tile contains a single land cover type. Datasets, such as land surface type, soil and vegetation parameters, model initialization, and atmospheric boundary conditions, are required as input data to apply CLM (Dai *et al.*, 2003). On the basis of the general mosaic concept, the energy and water balances are calculated for each time step in each tile (Koster and Suarez, 1992). The energy and water balance solution for each time step is conserved and integrated by an implicit time-integration scheme. The core single column soil–snow–vegetation bio-physical code is based on the governing equations of physical processes, including the water mass balance

equation (Equation (1)) and the energy (heat) conservation equation (Equation (2)) described as

$$\frac{\partial}{\partial t} \int_{\Delta V} \rho_k \theta_k dV = - \int_S U_k \cdot dS + \sum_{k'} \int_{\Delta V} M_{k'k} (1 - \delta_{k'k}) dV + \int_{\Delta V} S_k dV \quad (1)$$

$$\frac{\partial}{\partial t} \sum_{k=i,l,v,d} \int_{\Delta V} \rho_k \theta_k h_k dV = - \sum_{k=i,l,v} \int_S U_k h_k \cdot dS + \int_S \lambda \nabla T \cdot dS + \int_{\Delta V} R dV \quad (2)$$

where ρ_k is the intrinsic density of constituent k (kg m^{-3}), θ_k is the partial volume of constituent k ($\text{m}^3 \text{m}^{-3}$), h_k is the specific enthalpy (J kg^{-1}), U_k is the mass flux ($\text{kg m}^{-2} \text{s}^{-1}$), $M_{k'k}$ is the phase change from phase k' to phase k ($\text{kg m}^{-3} \text{s}^{-1}$), $\delta_{k'k}$ is the Kronecker delta, S_k is the source or sink term, λ is the thermal conductivity of the medium ($\text{W m}^{-1} \text{K}^{-1}$), and R is the radiation flux (W m^{-2}).

CLM can be viewed as a highly practical model due to its relatively simple parameterizations. The only required parameters are longitude, latitude, soil texture profile (percentage of sand/clay/loam), soil color index, and percentages of land cover types based on the International Geosphere–Biosphere Programme (IGBP) land cover classification. The model-forcing data includes downward solar radiation, downward longwave radiation, air temperature, wind speed, atmospheric pressure, specific humidity, and precipitation. The general patterns of the model-forcing data are shown in Figure 2, illustrating typical weather patterns occurring at the Haenam KoFlux site during the growing season: a large variation of downward solar radiation ($0\text{--}900 \text{ W m}^{-2}$) compared with the relatively constant longwave radiation ($400\text{--}450 \text{ W m}^{-2}$) and air temperature ranging from 295 and 303 K. As expected, attenuation of radiations and air temperature occurred during the rainfall events characterized by the Asian monsoon climate.

The soil texture parameters used in CLM to represent this study site were sand ($\sim 38.5\%$) and clay ($\sim 30.0\%$). Within the study area, sand percentages shrank, while clay percentages rose with increased soil depth. This soil information was obtained from the Rural Development Administration (<http://asis.rda.go.kr/>). Vegetation parameters used for CLM in the cropland are given in Table II. All vegetation parameters such as vegetation structure (i.e. root depth and leaf area index) in CLM are predetermined by the IGBP land cover classification. In this study, the IGBP 'cropland' classification was initially used to estimate energy and water balances in a single-point field because cropland is a prevailing land cover for this study area. Model simulations were initialized with sub-surface soil temperature and moisture values by the Haenam KoFlux site on 23 June.

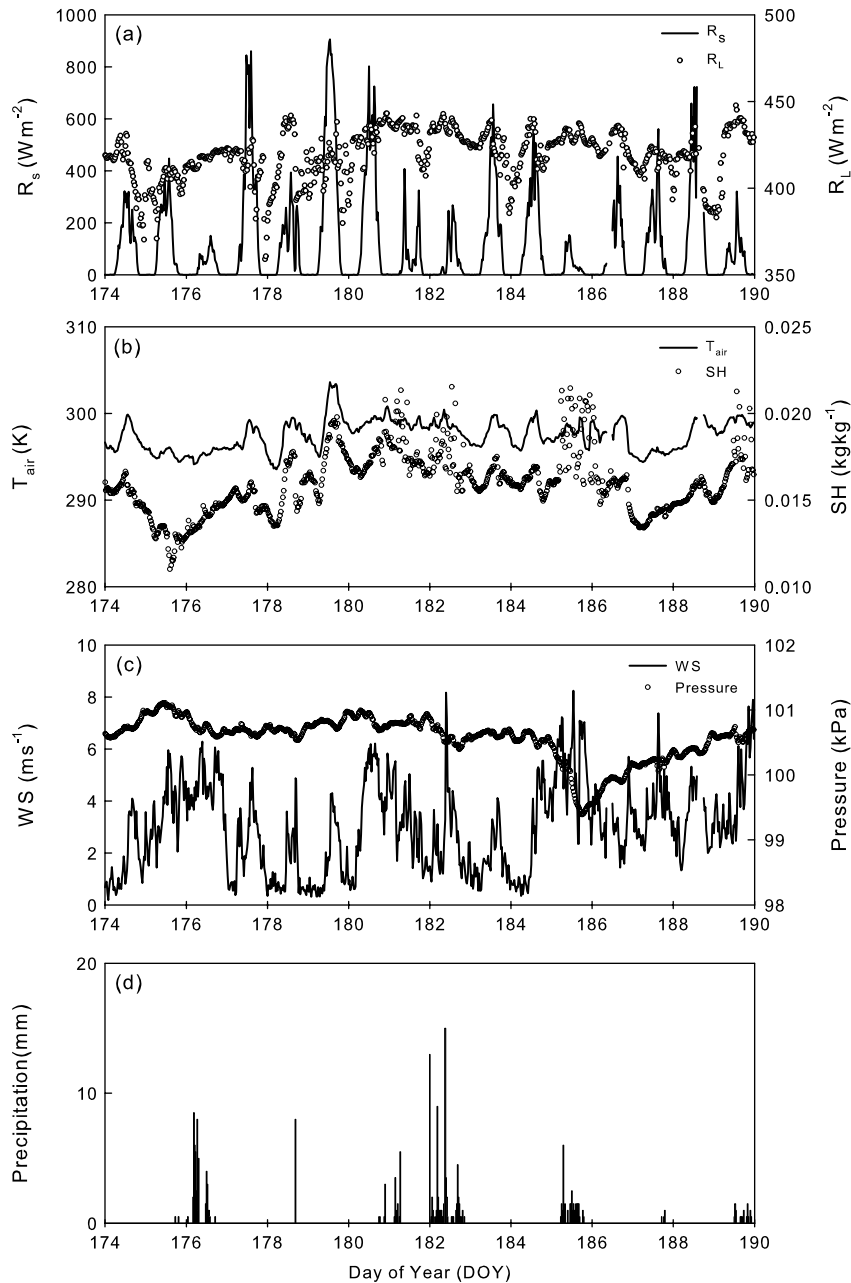


Figure 2. Time series of Common Land Model (CLM) forcing data of (a) the downward solar radiation (R_s) and the downward longwave radiation (R_L), (b) air temperature (T_{air}) and specific humidity (SH), (c) wind speed (WS) and pressure, and (d) precipitation

Table II. Soil and vegetation parameterization of cropland in Common Land Model (CLM)

Parameters	CLM
Soil texture	User defined
Porosity	User defined
Saturated hydraulic conductivity	Clapp and Hornberger (1978)
Thermal conductivity	Clapp and Hornberger (1978)
Wilting point	User defined
Water retention curve	Clapp and Hornberger (1978)
Root depth	0.2–0.6 m
Leaf area index	0.50–6.00
Canopy height	0.01–1.5 m
Roughness length	0.06 m

RESULTS AND DISCUSSION

Error assessment methods

The estimations of CLM in water and energy fluxes were evaluated through a comparison with the corresponding observed data using two different statistics. The two main statistics, Bias and root mean squared error (RMSE), used in this study are described as follows:

$$\text{Bias} = \frac{\sum_{i=1}^n (x_{\text{measured},i} - x_{\text{calculated},i})}{n} \tag{3}$$

$$RMSE = \sqrt{\frac{\sum_{i=1}^n (x_{measured,i} - x_{calculated,i})^2}{n}} \quad (4)$$

Water fluxes

The observed soil temperature and soil moisture at a depth of 10 cm were compared with the simulated soil temperature and soil moisture, which were weight-averaged from the top four layers (0–10 cm) to match with the measurement depth. The simulated soil temperature was lower (i.e. Bias value of 1.44 K) than the observed soil temperature (Figure 3) but had diurnal fluctuation patterns similar to those seen in the observations. The simulated soil temperature was likely more sensitive to this, resulting in more temporal fluctuation compared to that in the observed soil moisture during the rainfall events (DOY185–187). Figure 4 shows the time line of the observed and simulated soil moisture during the study period. The soil moisture exhibited the dry-down patterns before the rainfall events such as those on June 26 (DOY 178). During the rainfall events, there was a rapid increase in the soil moisture, which resulted in a decrease in the soil temperature. The temporal pattern of the simulated soil moisture generally agreed well with that of the

observed soil moisture. Regression constants, *a* and *b* (i.e. slope *a* close to 1.0 and intercept *b* close to zero) were estimated to be 0.99 and –0.11 with an *R*² value of 0.81. However, there were significant differences in the magnitudes between the simulated and observed soil moisture. The modelled soil moisture was underestimated compared to the measured soil moisture, showing the average values of the modeled and measured soil moistures to be 0.40 and 0.29 m³ m^{–3} respectively. The tendency of the model underestimation has been noted in several previous studies (Mohr *et al.*, 2000; Dai *et al.*, 2003; Whitfield *et al.*, 2006). They all demonstrated that the simulated soil moisture showed somewhat drier patterns compared to the measured soil moisture, even if it followed a reasonable temporal pattern with that of the measured soil moisture. In this study, the lower magnitudes of the simulated soil moisture were likely due to inappropriate land cover parameterization and soil texture, which may not reflect the actual field conditions properly. On the basis of the footprint analysis, which determines the source area of the fluxes (Kwon *et al.*, 2009), the land cover types of the study area, with heterogeneous mosaic patchiness, were reinvestigated using Landsat 7 land cover classification obtained from national water resources management systems in Korea (<http://www.wamis.go.kr>). Within the footprint area, the area was composed of 3% urban, 1.75% bare soil, 6.25% grass, 26.5% forest, 43.75% rice paddy, and 18.75% cropland. The actual measurements of the soil temperature and soil moisture were conducted at the borders between the mixed land covers, such as different agricultural crop types. Misrepresentation of the actual measurements and simple parameterization of land cover type and soil texture may be a cause of the discrepancies in soil temperature and moisture. Therefore, further studies on accurate parameterization are needed to provide better model performance.

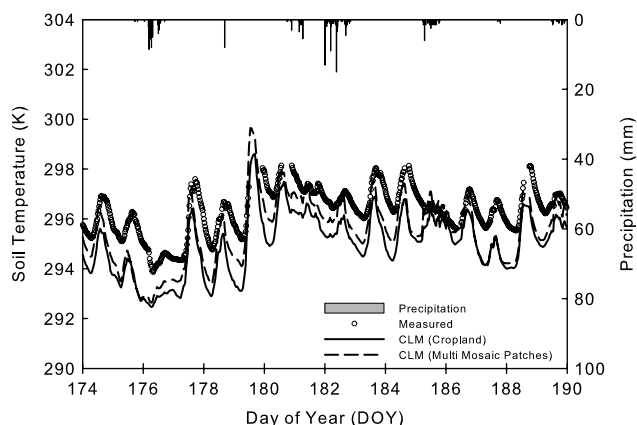


Figure 3. Time series of the measured and calculated soil temperature for 23 June–8 July, 2006

Energy fluxes

There was a fairly good agreement between the measured and calculated net radiations (Figure 5), although the calculated net radiation slightly underestimated the measured net radiation for the study period: Bias and

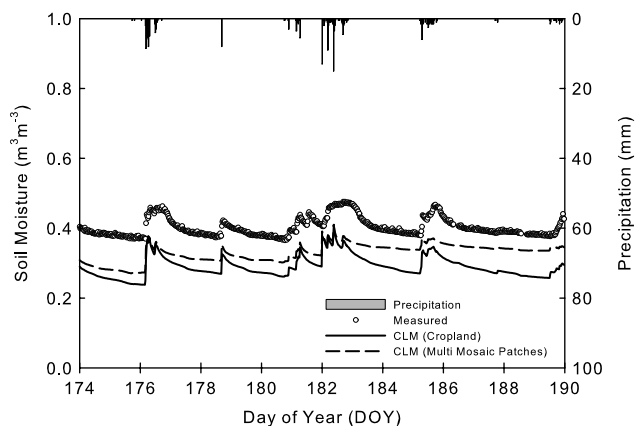


Figure 4. Time series of the measured and calculated soil moisture for 23 June–8 July, 2006

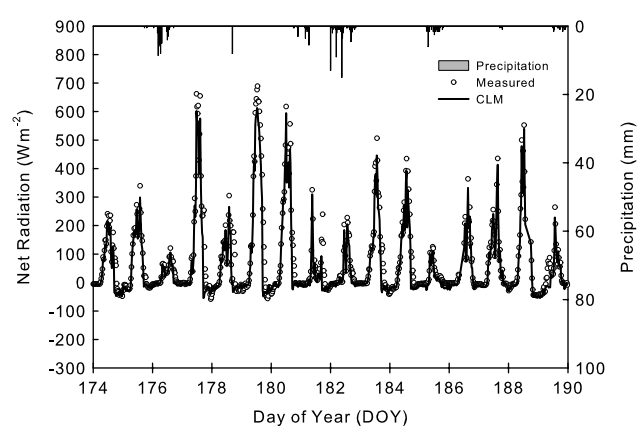


Figure 5. Comparison of the measured and calculated net radiation for 23 June–8 July, 2006

Table III. Comparison of statistics between the modelled and the actual measurements (Note: $Y = ax + b$: x = measurement and y = calculation)

IGBP	Variables ^a	Observed	Statistics					
			Average	Average	Bias	RMSE	a	b
Cropland	Soil temperature	296.28	294.97	1.44	1.55	1.04	-12.31	0.75
	Soil moisture	0.40	0.29	0.11	0.11	0.99	-0.11	0.81
	R_N	77	58	18	41	0.89	-9.79	0.93
	G	2	14	-14	24	2.51	11.00	0.52
	H	10	-11	21	66	1.99	-30.46	0.62
	LE	57	55	8	60	0.53	18.61	0.39
Multi mosaic patches	Soil temperature	296.28	295.49	0.93	1.15	1.08	-26.03	0.70
	Soil moisture	0.40	0.33	0.07	0.08	0.66	0.07	0.46
	R_N	77	62	15	39	1.00	-14.49	0.94
	G	2	16	-16	28	2.48	13.23	0.43
	H	10	-17	27	106	2.72	-44.52	0.55
	LE	57	63	13	64	0.49	16.32	0.34

^a Units of the variables are (K) for soil temperature, ($\text{m}^3 \text{m}^{-3}$) for soil moisture, (W m^{-2}) for net radiation (R_N), ground heat flux (G), sensible heat flux (H), and latent heat flux (LE).

RMSE were 18 and 41 W m^{-2} respectively and regression constants a and b were 0.89 and -9.79 respectively, with an R^2 value of 0.93 (Table III). This fairly good agreement for the net radiation resulted from reasonable estimates of albedo, reflected solar radiation, and upwelling longwave radiations in the model calculations (data not shown).

Even if the simulated sensible heat flux had a similar temporal pattern as that seen in the observed sensible heat flux, the former had larger values than the latter during mid-day and had negative values during rainfall events (Figure 6). The error statistics for the CLM was a bias of 21 W m^{-2} and an W m^{-2} RMSE of 66 W m^{-2} for the sensible heat flux and a bias of 8 W m^{-2} and a RMSE of 60 W m^{-2} for the latent heat flux (Table III). The estimation of the latent heat flux showed a better agreement with the observations than the sensible heat flux in both the magnitudes and temporal patterns (Figure 7). However, the simulated latent heat fluxes were overestimated; these were higher than the observed latent heat fluxes during the rainfall events. These patterns were likely not due to infiltration of moisture to soils, but rather

due to immediate evapotranspiration into the atmosphere, resulting in higher latent heat fluxes during the rainfall events. Underestimation of the sensible heat fluxes during rainfall events might be induced by the maintenance of the energy balance in CLM. Dickinson and Henderson-Sellers (1988) noted that the general circulation model (GCM), which was incorporated into CLM, computed a large negative sensible heat flux up to several hundred W m^{-2} when the latent heat flux exceeded the net radiation on tropical forest sites. These discrepancies can also be explained by particular climate conditions for the study area. Kang *et al.* (2009) demonstrated that measured heat fluxes decreased by seasonal depression associated with reduced available energy balance during summer monsoon. Watanabe and Mizutani (1996) noted that model comparison was not good during the rainfall events, predicting extremely large negative sensible heat flux, at forest sites in Japan.

These larger discrepancies in the simulated sensible heat flux were reported in several previous studies that applied different types of SVAT models (Liang *et al.*, 1998; Chang *et al.*, 1999; Whitfield *et al.*, 2006). Liang

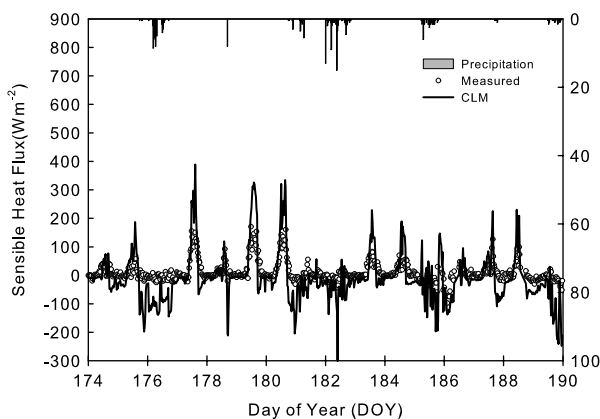


Figure 6. Comparison of the measured and calculated sensible heat flux for 23 June–8 July, 2006

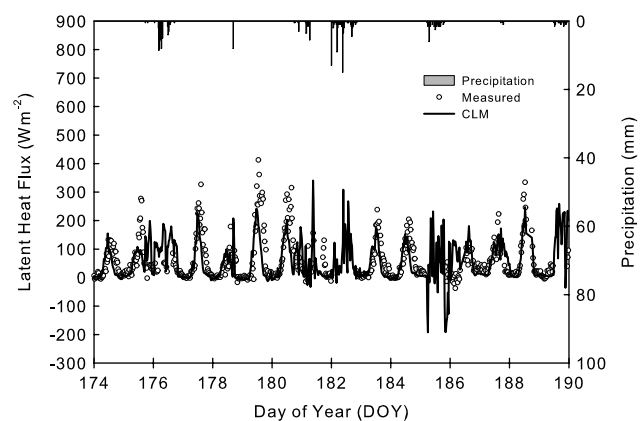


Figure 7. Comparison of the measured and calculated latent heat flux for 23 June–8 July, 2006

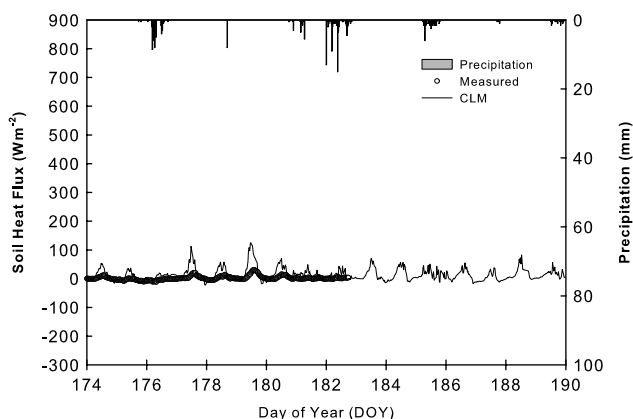


Figure 8. Comparison of the measured and calculated soil heat flux for 23 June–8 July, 2006

et al. (1998) demonstrated that spatial patterns of sensible and latent heat fluxes were estimated with relatively larger errors compared to that of net radiation. Chang *et al.* (1999) and Whitfield *et al.* (2006) noted that latent heat fluxes were better predicted compared to the sensible heat flux using the coupled atmosphere plant soil (CAPS) model along with the CLM. These identified patterns for the heat fluxes indicate that the CLM parameterizations for the latent heat flux seem to be more physically comprehensive than model parameterizations for the sensible heat flux.

There were significant differences between the simulated and the observed soil heat flux (Figure 8). In the CLM, the soil heat flux was computed as the residual of the energy balance equation (ground heat flux = net radiation – sensible heat flux – latent heat flux; Dai *et al.*, 2003). Compared to the observed ground heat flux, the larger values of the simulated ground heat flux indicate the embedded errors in the estimation of sensible heat flux and latent heat flux on the simulated ground heat flux.

The energy balance closure has been shown, in Figure 9, to examine the performance of the energy fluxes in the CLM. The energy balance closure was close to 1.0, except during the times for rainfalls. Unlike the result of

the energy closure from the CLM, the energy balance closure of the measurements was close to 0.92, but it showed occasionally high values.

Sensitivity test

Alteration of the parameterization schemes (e.g. land cover types and soil texture) may result in different estimations of the water and energy fluxes. We have investigated how much the model performances were affected by the different land cover types. In order to consider the heterogeneity of the study site, the cropland of the IGBP land cover classification was modified to the multi-mosaic patches mentioned earlier. The average values of the soil temperature and soil moisture were closer to the measurements, that is, 295.49 K and 0.33 m³ m⁻³ (Figure 4), and the error statistics, bias, and RMSE had improved to 0.93 and 1.15 K and 0.07 and 0.08 m³ m⁻³ respectively. However, the regression constants *a* and *b* were somewhat poorly estimated (Table III). For energy fluxes, the net radiation estimation had improved, but other components for the energy balance remained unchanged or were slightly worse compared to the cropland parameterization (Table III).

We also examined the influence of soil texture alteration (i.e. sand and clay percentages) on the model performance. Sand and clay percentages in the soil texture had altered in ±10% increments up to ±50%. While soil moisture and turbulent fluxes tended to change slightly (approximately 2.3% for soil moisture and 0.5% for sensible heat flux) along with entire range of the clay percentage increase, relatively consistent patterns were seen in the soil temperature and the latent heat flux (Figures 10 and 11). Within the range of the sand percentage variation, these variables tended to decrease. In both the cases of the sand percentage alterations, the soil moisture had changed by about 12%, while the soil temperature and heat fluxes had changed by only about 1%. This result was concurrent with that of the different land cover schemes. Unlike Peters-Lidard *et al.* (1998) and Mohr *et al.* (2000), who reported the effect of soil type specifications on soil moisture and turbulent fluxes, the result

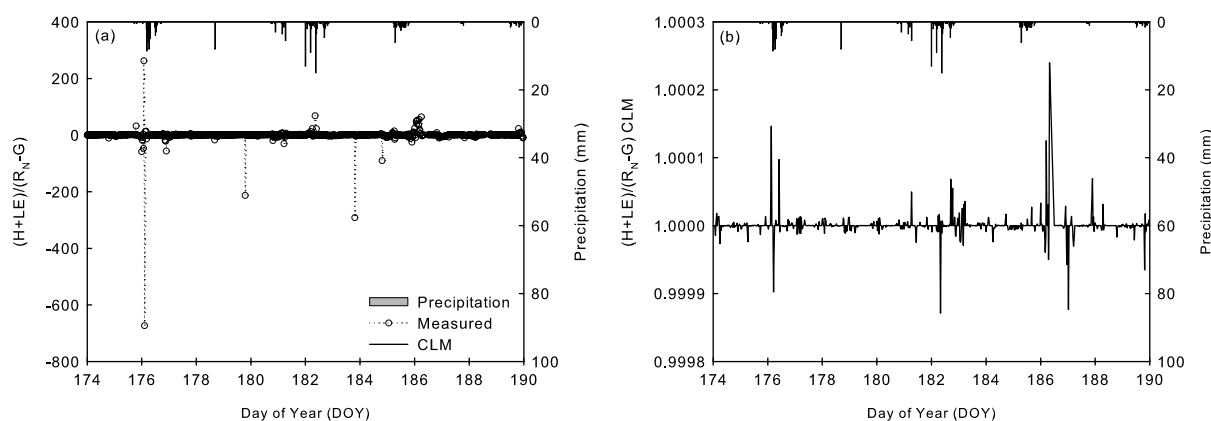


Figure 9. Comparison of the measured and calculated energy balance ratio (i.e. the ratio of the sum of sensible and latent heat fluxes to the sum of net radiation and ground heat flux: $(H + LE)/(R_N - G)$) for 23 June–8 July, 2006: (a) the measured and calculated energy balance ratio and (b) the calculated energy balance ratio (note for a different scale)

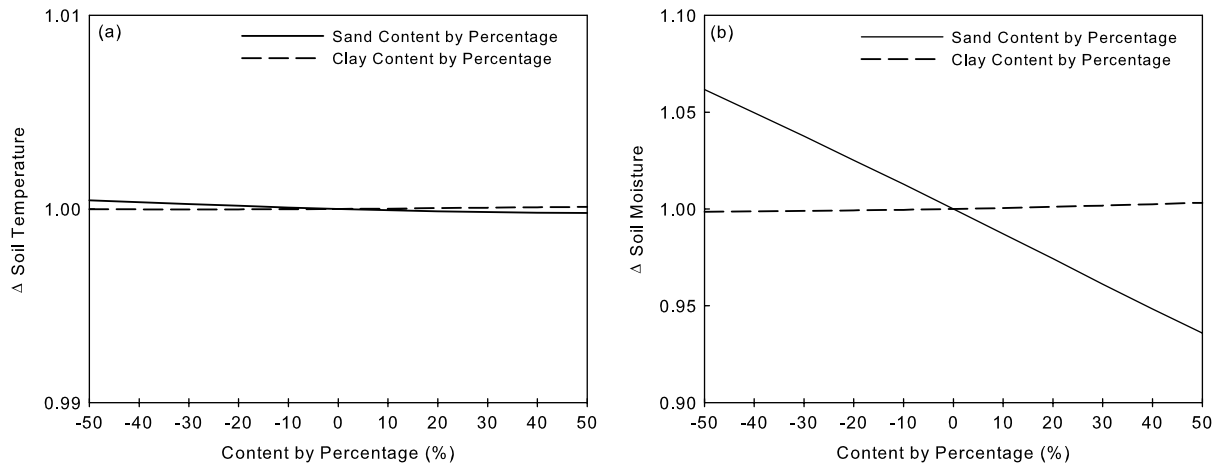


Figure 10. Sensitivity test of soil temperature (a) and soil moisture (b) with the changes of sand and clay percentage ($\pm 50\%$ with a 10% increment) in soil texture (note for the different scales of (a) and (b))

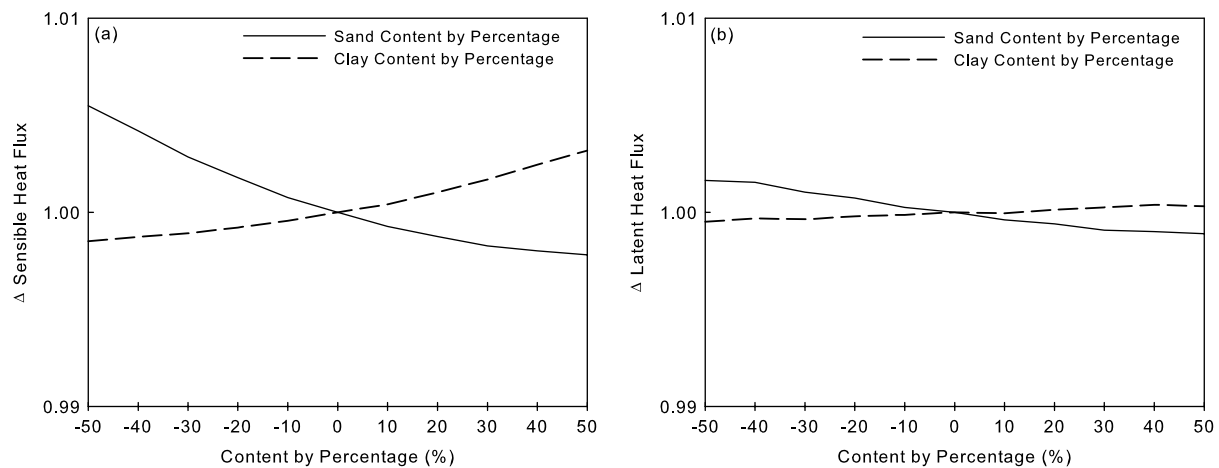


Figure 11. Sensitivity test of sensible heat flux (a) and latent heat flux (b) with the changes of sand and clay percentage ($\pm 50\%$ with a 10% increment) in soil texture

in this study showed the influence of soil texture on soil moisture but not on turbulent fluxes.

CONCLUSION

In this study, we used CLM to replicate the water and energy fluxes on a typical farmland in Korea. The results indicate that CLM can be used to reasonably estimate the water and energy balance within allowable error ranges without optimization. While the simulated soil moisture was similar to that observed with respect to temporal variations, it was relatively underestimated when compared to the observed using the simple IGBP land cover parameterization (cropland). Additionally, the modification of the IGBP land cover classification with heterogeneous mosaic patches improved the estimations of soil temperature, soil moisture, and net radiation. However, there was no improvement in the sensible and latent heat fluxes, even after modification of the IGBP land cover classification. Alteration of the soil texture parameterization also produced similar results to those of the land cover modification. On the basis of this study, which initially employed CLM in Korea, further

model parameterization and a realistic initialization could provide a more accurate estimation of water and energy fluxes.

ACKNOWLEDGEMENTS

This work was supported by the research fund of Hanyang University (HY-2009-N). The data were provided by KoFlux from the projects funded by the Ministry of Land, Transport and Maritime Affairs, the Korea Forest Research Institute, and the Korea Science and Engineering Foundation. Thanks to graduate student, Ji-Woong Jin, Hongik University for his assistance.

REFERENCES

- Baldocchi D, Falge E, Gu L, Olson R, Hollinger D, Running S, Anthoni P, Bernhofer Ch, Davis K, Evans R, Fuentes J, Goldstein A, Katul G, Law B, Lee X, Malhi Y, Meyers T, Munger W, Oechel W, Paw UKT, Pilegaard K, Schmid HP, Valentini R, Verma S, Vesala T, Wilson K, Wofsy S. 2001. FLUXNET: a new tool to study the temporal and spatial variability of ecosystem scale carbon dioxide, water vapor, and energy flux densities. *Bulletin of the American Meteorological Society* **82**: 2415–2434.

- Beven KJ, Kirkby MJ. 1979. A physically based variable contribution area model of basin hydrology. *Hydrological Science Bulletin* **24**: 43–69.
- Chang S, Hahn D, Yang CH, Norquist D. 1999. Validation study of the CAPS model land surface scheme using the 1987 Cabauw/PILPS dataset. *Journal of Applied Meteorology* **38**: 405–422.
- Choi M, Jacobs JM, Bosch DD. 2008. Remote sensing observatory validation of surface soil moisture using advanced microwave scanning radiometer E, common land model, and ground based data: case study in SMEX03 Little River Region, Georgia, U.S. *Water Resources Research* **44**: W08421. DOI:10.1029/2006WR005578.
- Clapp RB, Hornberger GM. 1978. Empirical equations for some soil hydraulic-properties. *Water Resources Research* **14**: 601–604.
- Dai Y, Zeng X, Dickinson RE, Baker I, Bonan GB, Bosilovich MG, Denning AS, Dirmeyer PA, Houser PR, Niu G, Oleson KW, Schlosser CA, Yang ZL. 2003. The common land model. *American Meteorological Society* **84**(8): 1013–1023.
- Dickinson RE, Henderson-Sellers A. 1988. Modeling tropical deforestation: a study of GCM land-surface parameterizations. *Quarterly Journal of Royal Meteorological Society* **114**: 439–462.
- Hong J, Kwon H, Lim JH, Byun YH, Lee J, Kim J. 2009. Standardization of KoFlux Eddy-covariance data processing. *Korean Journal of Agricultural and Forest Meteorology* **2**: 19–26.
- Kang M, Park S, Kwon H, Choi H, Choi Y, Kim J. 2009. Evapotranspiration from a deciduous forest in a complex terrain and a heterogeneous farmland under monsoon climate. *Asia-Pacific Journal of Atmospheric Science* **45**(2): 175–191.
- Kim J, Kim W, Cho CH, Choi BC, Chung HS, Lee BL, Kim KH, Kim KR, Kim MY, Lee BY, Lee GW, Lee JT, Lim JH, Oh HH, Park EW, Shim JS, Yun JI, Rho CS. 2002. *KoFlux: A new tool to study the biosphere-atmosphere interactions in Asia*. In: Lee D, Jin V, Son Y, Yoo S, Lee HY, Hong SK, Ihm BS (eds) Ecol of Korea. Bumwoo Publishing Company: Seoul; 215–229.
- Koster RD, Suarez MJ. 1992. Modeling the land surface boundary in climate models as a composite of independent vegetation stands. *Journal of Geophysical Research: Atmosphere* **97**(D3): 2697–2715.
- Kumar SV, Peters-Lidard CD, Tian Y, Houser PR, Geiger J, Olden S, Lighty L, Eastman JL, Doty B, Dirmeyer P, Adams J, Mitchell K, Wood EF, Sheffield J. 2006. Land information system—an interoperable framework for high resolution land surface modeling. *Environmental Modeling and Software* **21**: 1402–1415.
- Kustas WP, Humes KS, Norman JM, Moran MS. 1996. Single-and dual-source modeling of surface energy fluxes with radiometric surface temperature. *Journal of Applied Meteorology* **35**(1): 110–121.
- Kwon H, Park S, Kang M, You J, Yuan R, Kim J. 2007. Quality control and assurance of eddy covariance data at the two KoFlux sites. *Korean Journal of Agricultural and Forest Meteorology* **9**: 260–267.
- Kwon H, Park TY, Hong J, Lim JH, Kim J. 2009. Seasonality of net ecosystem carbon exchange in two major plant functional types in Korea. *Asia-Pacific Journal of Atmospheric Sciences* **45**(2): 149–163.
- Lee HC, Hong JK, Cho CH, Choi BC, Oh SN, Kim J. 2003. Surface exchange of energy and carbon dioxide between the atmosphere and a farmland in Haenam, Korea. *Korean Journal of Agricultural and Forest Meteorology* **5**(2): 61–69.
- Lee Y, Kim J, Hong J. 2008. The simulation of water vapor and carbon dioxide fluxes over a rice paddy field by modified Soil-Plant-Atmosphere Model (mSPA). *Asia-Pacific Journal of Atmospheric Sciences* **44**(1): 69–83.
- Liang X, Wood EF, Lettenmaier DF, Lohmann D, Boone A, Chang S, Chen F, Dai Y, Desborough C, Dickinson RE, Duan Q, Ek M, Gusev YM, Habets F, Irannejad P, Koster R, Mitchell KE, Nasonova ON, Noilhan J, Schaake J, Schlosser A, Shao Y, Shmakin AB, Verseghy D, Warrach K, Wetzel P, Xue Y, Yang Z, Zeng Q. 1998. The project for intercomparison of land-surface parameterization schemes (PILPS) phase-2c Red-Arkansas river basin experiment: 2. Spatial and temporal analysis of energy fluxes. *Global and Planetary Change* **19**(1–4): 137–159.
- Lohmann D, Lettenmaier DP, Liang X, Wood EF, Boone A, Chang S, Chen F, Dai Y, Desborough C, Dickinson RE, Duan Q, Ek M, Gusev YM, Habets F, Irannejad P, Koster R, Mitchell KE, Nasonova ON, Noilhan J, Schaake J, Schlosser A, Shao Y, Shmakin AB, Verseghy D, Warrach K, Wetzel P, Xue Y, Yang Z, Zeng Q. 1998. The project for intercomparison of land-surface parameterization schemes (PILPS) phase-2c Red-Arkansas river basin experiment: 3. Spatial and temporal analysis of water fluxes. *Global and Planetary Change* **19**(1–4): 161–179.
- Mohr KI, Famiglietti JS, Boone A, Starks PJ. 2000. Modeling soil moisture and surface flux variability with an untuned land surface scheme: A case study from the Southern Great Plains 1997 Hydrology Experiment. *Journal of Hydrometeorology* **1**: 154–169.
- Moulin S, Bondeau A, Delecolle R. 1998. Combining agricultural crop models and satellite observations: from field to regional scales. *International Journal of Remote Sensing* **19**(6): 1021–1036.
- Peters-Lidard CD, Blackburn E, Liang X, Wood EF. 1998. The effect of soil thermal conductivity parameterization on surface energy fluxes and temperatures. *Journal of Atmospheric Sciences* **55**: 1209–1224.
- Watanabe T, Mizutani K. 1996. Model study on micrometeorological aspects of rainfall interception over an evergreen broad-leaved forest. *Agricultural and Forest Meteorology* **80**: 195–214.
- Whitfield B, Jacobs JM, Judge J. 2006. Intercomparison study of the land surface process model and the common land model for a prairie wetland in Florida. *Journal of Hydrometeorology* **7**(6): 1247–1258.
- Wilczak JM, Oncley SP, Stage S. 2001. Sonic anemometer tilt correction algorithms. *Boundary-Layer Meteorology* **99**: 127–150.
- Yang Z, Dickinson RE, Henderson-Sellers A, Pitman A. 1995. Preliminary study of spin-up processes in land surface models with the first stage data of Project for Intercomparison of Land Surface Parameterization Schemes Phase 1(a). *Journal of Geophysical Research* **100**(D8): 16553–16578.